Development of Fiber Bragg Grating Strain Amplification Sensor For Use In Nuclear Power Plants

Jack Marston
Electronic and Electrical Engineering Department
University of Strathclyde
Glasgow, United Kingdom
jack.marston@strath.ac.uk

Grzegorz Fusiek
Electronic and Electrical Engineering Department
University of Strathclyde
Glasgow, United Kingdom
g.fusiek@strath.ac.uk

Paweł Niewczas
Electronic and Electrical Engineering Department
University of Strathclyde
Glasgow, United Kingdom
p.niewczas@strath.ac.uk

Jiansong Guo
Civil Design Group
EDF Energy
Glasgow, United Kingdom
jiansong.guo@edf-energy.com

Abstract— **This paper outlines the motivation for structural health monitoring with fiber Bragg grating (FBG) strain sensors in nuclear power plants where a high measurement resolution is normally required. Hence, a mechanical strain amplification is needed to increase the strain sensitivities. To ensure long-term stability, an epoxy-free mechanical strain amplification sensor is constructed using a Kovar encapsulated FBG. The strain response of the sensor is characterized using an extensometer. It was found that the achieved sensitivity of 1.16 ± 0.008 pm/με yields a strain resolution of 0.43 ± 0.003 με with current interrogation method – which exceeds the required strain resolution for the postulated scenario. However, if a higher resolution is required, it can be achieved by using an interrogator with a higher wavelength resolution or using a strain amplification with a larger strain amplification coefficient.**

Index Terms—**optical strain sensing, nuclear power plant, mechanical strain amplification, fiber Bragg grating sensors, metal encapsulation of fiber Bragg gratings.**

I. INTRODUCTION

Nuclear power plants are comprised of a reactor surrounded by pre-stressed concrete containment vessels. These containment vessels are important, given that they protect the reactor and help prevent radioactive material from being released into the environment. Due to the long life of nuclear power plants (50+ years), it is important to monitor the structural health of the concrete during the lifetime of the plant and into the decommissioning phase. Currently, this is done largely by manual inspection of the concrete structures. Alternatively, remotely operated drones can be used to identify surface cracks [1], [2]. Either method is costly, time consuming and incapable of detecting internal structural changes in the concrete. As a result, a structural health monitoring system would be preferred, ideally indicating also internal changes in the concrete, e.g., through surface strain monitoring. Photonic based strain sensors have been identified as a good candidate for such a structural health monitoring system, specifically FBGs, due to their excellent multiplexing capabilities and, as with all optical sensors, immunity to electromagnetic interference. FBGs also have superior strain resolution to distributed fiber-optic strain sensors based on the Brillouin scattering mechanism [3].

FBG sensors have begun to be used in a wide array of structural health monitoring tasks in a variety of industries including nuclear [4]– [6] and civil engineering [7]–[9]. Such applications often involve placing the sensors in harsh industrial environments that are exposed to varying temperature, moisture, chemical contamination, etc. Additionally, the applications often have a long lifetime requirement from the sensor solution. Traditionally such FBGs have been bonded to a substrate using epoxies [10], [11]; however, these tend to swell when exposed to moisture and thus are unsuited to outdoor use [9].

Previous work involved creating a packaging method based on sealing a metal coated fiber inside a Kovar capillary by induction brazing [12], [13]. This packaging method eliminates the influence of moisture on the sensor performance as well as providing an armor around the FBG to protect it from damage and making the solution well suited to harsh industrial environments. Such Kovar encapsulated FBGs have been used in structural health monitoring for both prestressed tendons in nuclear power plants [14], [15] as well as in wind turbine foundations [16], [17]. However, here we require a greater strain resolution than these applications to detect strain changes in the prestressed concrete containment vessel (PCCV) and hence mechanical strain amplification is proposed to increase the sensitivity of the sensors. This paper covers a novel arrangement and construction of a Kovar-packaged FBG sensor with a mechanical strain amplification and reports on the strain response characterization of the sensor using a stressing machine.

II. THEORY

A. Fibre Bragg Gratings

FBGs are constructed by using UV-light to inscribe a periodic modulation to the refractive index in an optical fiber. When illuminated with a broadband laser a specific wavelength is reflected by the FBG at the Bragg wavelength, λ_B. The peak wavelength is described by the following relationship:

$$\lambda_B = 2n_{eff}\Lambda \tag{1}$$

where n_{eff} is the effective refractive index of the fiber and Λ is the grating period. Thus, the wavelength is temperature dependent (as refractive index is temperature dependent) and strain dependent, as the grating period vary with stretching/compressing the fiber.

A relative change in FBG peak wavelength can be described as

$$\frac{\Delta\lambda_B}{\lambda_B} = C_k\Delta\varepsilon + C_T\Delta T \qquad (2)$$

where C_k is strain sensitivity and C_T, temperature sensitivity.

As such the strain and temperature will need to be decoupled to provide strain only measurements as FBGs are dependent on both. This can be readily achieved by adding a second FBG in thermal contact with the strain sensor such that it is not mechanically coupled and does not elongate/compress when load is applied [10], [18].

B. Strain Resolution Calculations

In nuclear power plants, the containment vessels are typically concrete hollow cylinders with a domed roof with steel tendons inside to reinforce the concrete. These tendons are prestressed to increase the load capacity of the concrete structure [19]. To demonstrate the magnitude of the strain resolution required for structural health monitoring of such structures, the strain change due to a single, vertical, tendon failure is considered. This is a highly simplified model, and the required resolution could be higher than presented, as it depends on many other factors, i.e., a forewarning is at least a preference, etc.

Tendons may undergo damage over time due to contact with water and corrosion, and thus corrosion failure remains a possibility. There are of course other failure modes that could be considered, for example internal cracking of the concrete structure, but the proposed failure mode could offer a 'general idea' of the magnitude for the required strain measurement at the surface of the concrete where the sensors can be mounted.

For this purpose, the prestressed concrete containment vessel (PCCV) in Ohi Nuclear Power Plant was considered with a diagram seen in Fig. 1 and values taken from [19]. Here there are two types of tendons, vertical tendons, and horizontal tendons. Only vertical tendon failure mode was considered. The outer diameter of the cylinder is 45 m and vertical tendons are prestressed to 7.05 MN. Assuming a wall thickness of 1.5 m and Young's modulus of concrete as 41 GPa by using the following simplified method:

$$\varepsilon = \frac{F_{pre}}{AE} \qquad (3)$$

where F_{pre} is the prestressing force of the tendon, A is the cross-sectional area of the concrete cylinder shell and E is the Young's modulus of the concrete, the strain change due to the failure of a tendon can be determined.

$$\varepsilon = \frac{7.05}{204.9503\times41} = 0.84 \text{ } \mu\varepsilon \qquad (4)$$

A tendon failure represents a large mode of failure and thus a strain resolution lower than this is better to monitor the structural health of the PCCV (as noted previously the value obtained here is only for a demonstration).

C. Mechanical Strain Amplification

Due to the small value of the strain being resolved, it was decided that a way of amplifying the strain may be needed for applications in the nuclear power plants. In order to achieve this, mechanical strain amplification was selected as the method, the theory of which is outlined below.
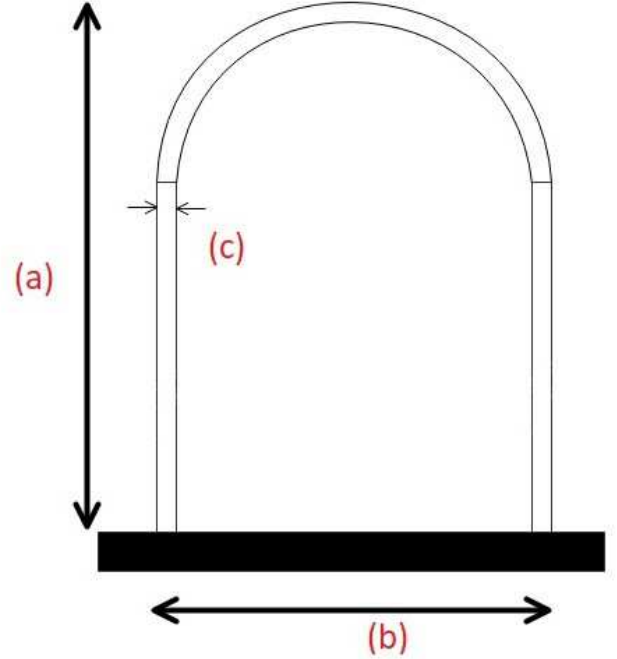

Fig. 1. Schematic cross-sectional elevation of the Ohi PCCV. Here the height of the PCCV is 65 m seen at (a), the outer diameter is 45 m seen at (b) and the thickness of the walls is 1.5 m seen at (c).
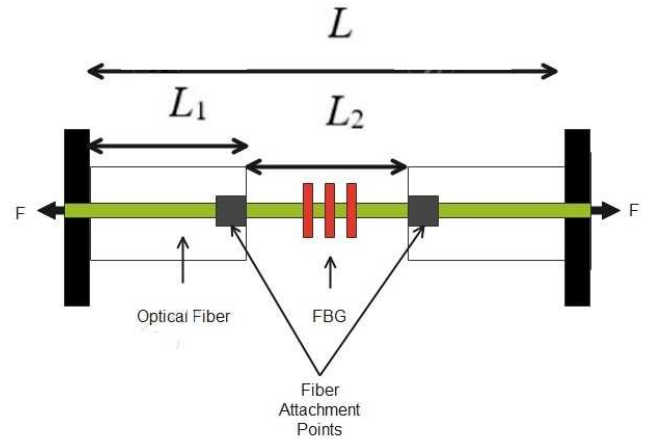

Fig. 2. Schematic outlining the principles underpinning strain amplification. With F showing the direction of applied load.

Consider the diagram in Fig. 2. Here an FBG of length L_2 suspended over a gap and attached to a steel plate of length L_1 at either end. When load F is applied along the axis of the

fiber, an elongation of ΔL is seen. The decompose of the elongation can be seen here:

$$\Delta L = 2\Delta L_1 + \Delta L_2 \qquad (5)$$

with ΔL_2, the elongation of the FBG and ΔL_1 the elongation of the plate. As the area of the fiber is so small compared to the plates, it is found from (3) and the definition of strain

$$\Delta L_1 \ll \Delta L_2 \qquad (6)$$

this implies that from (5) and (6)

$$\Delta L \approx \Delta L_2 \qquad (7)$$

this implies

$$\varepsilon^{'} = \frac{\Delta L}{L_2} \qquad (8)$$

where ε' is the strain of the sensor. This implies the strain amplification coefficient k is given by:

$$k = \frac{\varepsilon^{'}}{\varepsilon} \approx \frac{\Delta L/L_2}{\Delta L/L} \approx \frac{L}{L_2} \qquad (9)$$

And so, the amplification factor is the ratio of total length to the length of the sensor. A full treatment of the theory can be found in [7].

III. SENSOR CONSTRUCTION

As seen in Fig 3, the sensor consists of a 195×56×2 ± 0.03 mm thick steel plate with a 75×36 ± 0.03 mm slot cut out the center. Two 85×34×1 ± 0.03 mm plates are then spot welded on to the top of the plate such that they are centered and hang over the slot and are free to move as the sensor undergoes stress. Here the uncertainty of the dimensions are taken from the accuracy of the calipers used to measure them. The steel used is SS304, with Young's modulus E = 190 ± 5 GPa. The gap between the two plates is three times the length of the slot to give a strain amplification coefficient of k = 3 ± 0.012. The uncertainty is calculated by standard uncertainty propagation. $L = 75 \pm 0.05$ mm and $L_2 = 25 \pm 1$ mm. Where the uncertainty of the large uncertainty in L_2 is due to the imprecise spot welding. All other lengths stated in this paper have an uncertainty of ± 0.03 mm apart from L_{con} which has an uncertainty of ± 1 mm again due to imprecise welding.

A copper coated FBG was encapsulated in a 30 mm Kovar capillary using induction brazing with silver paste to steel shims, similar to the process described here [12], [13]. The FBG was prestressed during the brazing process to prevent "slacking" of the fiber inside the capillary. The shims were then spot welded to the steel plates across the gap (see Fig. 3). In addition, two copper-coated reference FBGs were attached to the steel frame. Two were epoxied with one at the side of the steel frame (i.e., not across the gap) and one across the gap. The purpose of the reference FBGs was to have independent measurements of strain, irrespective of the machine's intrinsic force and elongation measurement capability.

IV. EXPERIMENT, RESULT AND DISCUSSION

The FBGs were interrogated using an I-MON 256 USB (Ibsen Photonics) and the extensometer machine used for strain characterization was a 10-kN Testometric M350-10CT tensioning machine with an oven attached to set a constant temperature. The machine has a force accuracy of 5 N, the figure given by the manufacturer.

In order to characterize the strain response of the sensor, it was placed in the machine grips (Fig 4). A cyclical load was applied starting at a 100 ± 5 N load to 1300 ± 5 N for ten cycles at a constant temperature of 30 ± 0.03 °C, with the uncertainty determined from the range of temperatures measured by a temperature probe within the oven when held at 30 °C. This temperature was selected as this was the minimum stable temperature of the oven available and is close to the expected operating temperature. This cycle was completed at a rate of 1 mm/min with a maximum extension of 0.197 mm. Therefore, each cycle took ≈ 24 s.

The wavelength and load cell voltage, linearly related to force, were both measured. Strain can be calculated by the following relation:

$$\varepsilon = \frac{F}{AE} \qquad (10)$$

with ε as strain, F the load applied, A the cross-sectional area and E the Young's modulus of steel. The strain can then be decomposed into the narrow section, ε_{narrow}, connector section, ε_{con}, and the wide sections, ε_{wide}, of the sensor (seen in Fig. 3). The connector section is due to the spot weld not being placed right at the edge of slot. Consider total elongation and its decomposition:

$$\Delta L_{tot} = \Delta L_{narrow} + 2\Delta L_{wide} + 2\Delta L_{con} \qquad (11)$$

where ΔL_{tot} is the total elongation, ΔL_{narrow} is the elongation of the narrow region, ΔL_{wide} is the elongation of the wide region, ΔL_{wide} is the elongation of the narrow region, ΔL_{con} is the elongation of the connector region. Now from the definition of strain:

$$\varepsilon = \frac{\Delta L}{L} \qquad (12)$$

by rearranging it is found that

$$\Delta L = \varepsilon L \qquad (13)$$

now from (10), (11) and (13) it is found that

$$\Delta L_{tot} = \frac{FL_{narrow}}{EA_{narrow}} + 2\frac{FL_{wide}}{EA_{wide}} + 2\frac{FL_{con}}{EA_{con}} \qquad (14)$$

with E as the Young's modulus of steel, L_{narrow}, L_{wide} and L_{con} the lengths of the narrow, wide and connector regions and A_{narrow}, A_{wide} and A_{con} the cross-sectional area of the narrow, wide, and connector regions. It is found that the total strain from (12) and (13) can be expressed as follows:

$$\varepsilon_{tot} = \frac{F}{EL_{tot}}\left(\frac{L_{narrow}}{A_{narrow}} + 2\frac{L_{wide}}{A_{wide}} + 2\frac{L_{con}}{A_{con}}\right) \qquad (15)$$

with ε_{tot} the total strain and L the length between the grips, and substituting the values it is found that

$$\varepsilon_{tot} = 129 \pm 2 \ \mu\varepsilon$$

The strain in the side epoxy can be found by considering the strain in the narrow region.

$$\varepsilon_{narrow} = \frac{F}{EA_{narrow}} \tag{16}$$

and it is found that

$$\varepsilon_{narrow} = 171 \pm 5 \ \mu\varepsilon$$

The strain across the Kovar capillary can be found by considering the elongation across the gap:

$$\Delta L_{gap} = \Delta L_{narrow} + 2\Delta L_{con} \tag{17}$$

Now from a similar calculation as above we find:

$$\varepsilon_{gap} = \frac{\Delta L_{gap}}{L_{gap}} = \frac{F}{EL_{gap}}\left(\frac{L_{narrow}}{A_{narrow}} + 2\frac{L_{con}}{A_{con}}\right) \tag{18}$$

So, once the values are substituted, it is found:

$$\varepsilon_{gap} = 518 \pm 0.4 \ \mu\varepsilon$$

the strain sensitivities can then be found:

$$S = \frac{\lambda_{max}}{\varepsilon} \tag{19}$$

with S the sensitivity and λ_{max} the maximum wavelength measured. So, it is found that

$$S_{epoxy} = \frac{\lambda_{max,narrow}}{\varepsilon_{narrow}} = \frac{200 \pm 0.5pm}{171 \pm 5\mu\varepsilon}$$
$$= 1.17 \pm 0.03 \ \text{pm/}\mu\varepsilon \tag{20}$$

and

$$S_{kovar} = \frac{\lambda_{max,gap}}{\varepsilon_{gap}} = \frac{603 \pm 0.5pm}{518 \pm 0.3\mu\varepsilon} = 1.16 \pm 0.008 \ \text{pm/}\mu\varepsilon \tag{21}$$

The uncertainty in the wavelength is taken as the resolution of IMON as the measurements were taken in a short time period. By plotting wavelength against total strain the strain amplification can be seen.
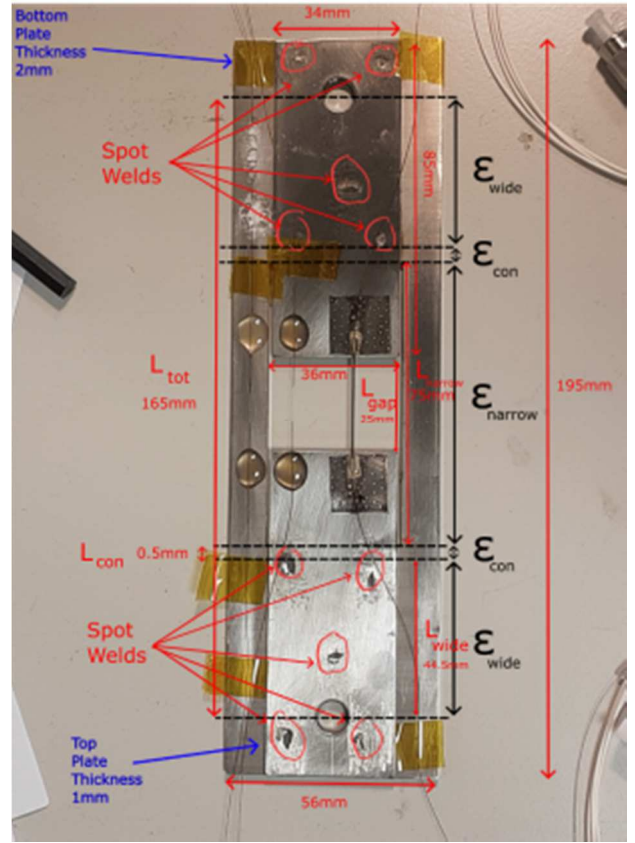

Fig. 3. A picture of the strain amplification sensor mounted with dimensions outlined and strain decomposition indicated.
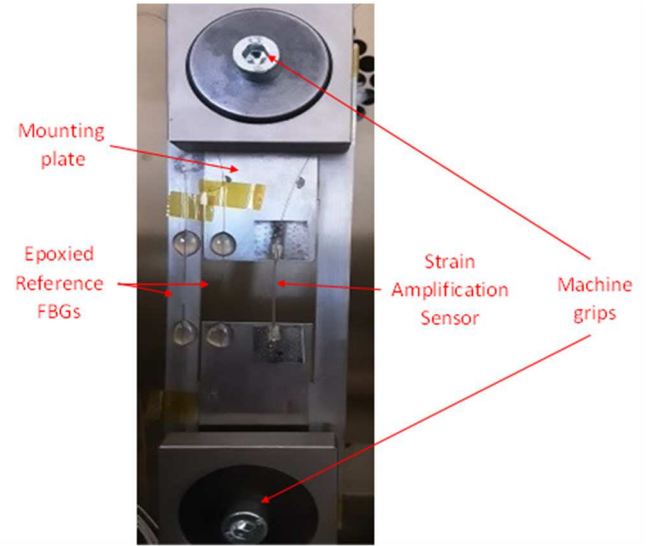

Fig. 4. A picture of the strain amplification sensor mounted in the extensometer. The two epoxied reference FBGs are on the left while the kovar capillary is on the right.
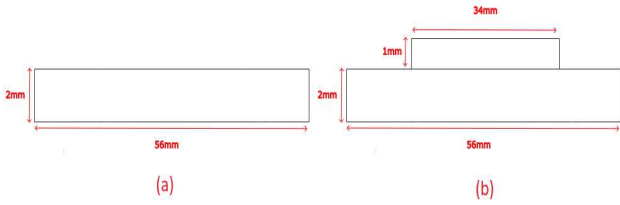
Fig. 5. Cross sectional areas of the connector region (a) and the wide region (b) of the sensor plates (crossection taken perpendicular to the straindirection).

Here the data from the side epoxy FBG and the Kovar encapsulated FBG will be analyzed and compared. In Fig. 6, it is evident that the strain response has a relatively tight hysteresis as well as being repeatable, i.e., traces a similar path each cycle for both the Kovar and side epoxy FBGs. A large hysteresis may affect the intended application as it would introduce an additional uncertainty between strain and wavelength; however, it is believed that the hysteresis is introduced by the stressing machine as it is visible in both the side epoxy and Kovar sensors – the Kovar sensor offering a clear amplification of the signal. The Kovar FBG has gradient of approximately three times the side epoxy FBG.
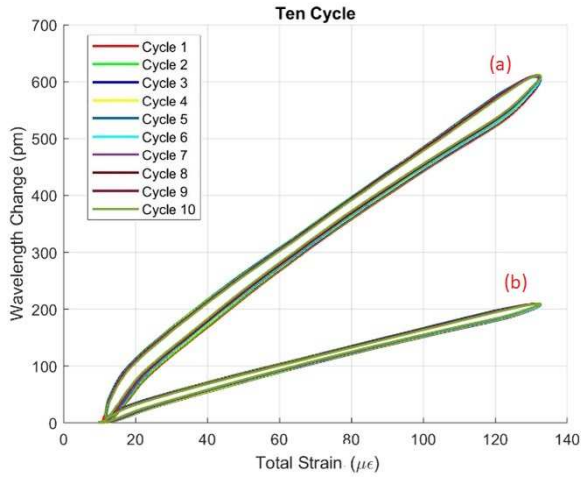

Fig. 6. Graph of wavelength against total strain. Loop (a) is from the kovar FBG and loop (b) is from the side epoxy FBG.

The sensitivity of the Kovar FBG was found to be 1.16 ± 0.008 pm/$\mu\varepsilon$ and the sensitivity of the side epoxy FBG, 1.17 ± 0.03 pm/$\mu\varepsilon$. The strain sensitivity for a bare fiber is 1.2 pm/$\mu\varepsilon$ [13]. This suggests the strain transfer for the epoxy is 97%. If the strain amplification coefficient of k = 3 ± 0.012 is considered, this means the strain sensitivity of the Kovar before amplification is 0.39 pm/$\mu\varepsilon$ and has a strain transfer ratio of 32%. This is similar to the work reported in [20]. Given the minimum wavelength resolution of 0.5 pm of the I-MON interrogator, this gives the minimum strain change detectable with the Kovar strain amplification of 0.43 ± 0.003 $\mu\varepsilon$ which is well below the minimum value calculated in section II B, suggesting that this sensor design will comfortably meet the resolution requirements for this application. Note that the amplification factor for the Kovar sensor was chosen arbitrarily to prove the principle of this approach. A greater amplification factor is readily achievable with this sensor design approach for applications that demand greater strain resolution.

V. CONCLUSION

The mechanical strain amplification functioned as anticipated, providing a boost to the sensitivity to bring it in line with the strain sensitivity of the epoxied FBG due to the poor strain transfer of the Kovar encapsulation. The minimum detectable strain of the amplification sensor operating with the current interrogation system was determined as 0.43 ± 0.003 $\mu\varepsilon$, well below the calculated minimum resolution value for the postulated prestressed concrete containment vessel measurement scenario. However, if a higher resolution is required, it can be achieved by using an interrogator with a higher wavelength resolution or using a strain amplification with a larger strain amplification coefficient. The rate of 1 mm/min the test was conducted at is greater than the rate that will be seen in the PCCV. However other tests carried out showed no significant difference in response when testing at lower rates. By considering the thermal strain in the FBG due to temperature variations of 0.03 °C, this results in a thermal strain of ε_{th} = 0.204 $\mu\varepsilon$, thus the uncertainty of the sensitivity may be underestimated due to thermal considerations. In the real-world application, a reference FBG will likely be deployed to provide temperature compensation. FBGs have a temperature sensitivity of 10.5 pm/°C which gives a temperature accuracy of 0.048 °C with the current optical setup. This level of uncertainty results in a thermal strain of ε_{th} = 0.33 $\mu\varepsilon$ [21], close to the sensitivity of the sensor.

Further work will investigate the temperature response of the sensor as well as the repeatability of the measurements. It is expected that the Kovar-encapsulated sensor will be immune to humidity changes that otherwise affect the epoxy bonded sensors.

REFERENCES

[1] Choi D, Bell W, Kim D, Kim J. UAV-Driven Structural Crack Detection and Location Determination Using Convolutional Neural Networks. *Sensors*. 2021; 21(8):2650.

[2] Li J, Li X, Liu K, Yao Z. Crack Identification for Bridge Structures Using an Unmanned Aerial Vehicle (UAV) Incorporating Image Geometric Correction. *Buildings*. 2022; 12(11):1869.

[3] A. Motil, A. Bergman, and M. Tur, '[INVITED] State of the art of Brillouin fiber-optic distributed sensing', *Optics & Laser Technology*, vol. 78, pp. 81–103, 2016.

[4] P. Niewczas, G. Fusiek, C. Lescure, M. Johnson, E. Iving, A. West, P. Crolla, and M. Walsh. Concept level evaluation of the full-scale deployment of fibre Bragg grating sensors for measuring forces in JET during plasma disruption events. In *Fifth International Conference on Condition Monitoring and Machine Failure Prevention Technologies ; Conference date: 15-07-2008 Through 18-07-2008*, 5 2008.

[5] Paul Crolla, Pawel Niewczas, and James R McDonald. An alternative method for the monitoring of strain and temperature in a nuclear fusion reactor. In *2009 44th International Universities Power Engineering Conference (UPEC)*, pages 1–4, 2009.

[6] Jung Ryul Lee, See Yenn Chong, Chang Yong Yun, and Hoon Sohn. Design of Fiber Bragg Grating Acoustic Sensor for Structural Health Monitoring of Nuclear Power Plant. In *Multi-Functional Materials and Structures III*, volume 123 of *Advanced Materials Research*, pages 859– 862. Trans Tech Publications Ltd, 12 2010.

[7] Hong-Nan Li, Dong-Sheng Li, and Gang-Bing Song. Recent applications of fiber optic sensors to health monitoring in civil engineering. *Engineering Structures*, 26(11):1647–1657, 2004.

[8] T H T Chan, L Yu, H Y Tam, Y Q Ni, S Y Liu, W H Chung, and L K Cheng. Fiber Bragg grating sensors for structural health monitoring of Tsing Ma bridge: Background and experimental observation. *Engineering Structures*, 28(5):648–659, 2006.

[9] Urszula Nawrot, Thomas Geernaert, Ben De Pauw, Dimitrios Anastasopoulos, Edwin Reynders, Guido De Roeck, and Francis Berghmans. Development of a mechanical strain amplifying transducer with Bragg grating sensor for low-amplitude strain sensing. *Smart Materials and Structures*, 26(7):75006, 6 2017.

[10] M. Perry, J. McAlorum, G. Fusiek, P. Niewczas, I. McKeeman, and T. Rubert, 'Crack Monitoring of Operational Wind Turbine Foundations', *Sensors*, vol. 17, 2017.

[11] J. McAlorum *et al.*, 'Comparison of epoxy and braze-welded attachment methods for FBG strain gauges', 12 2017.

[12] Grzegorz Fusiek, Tim Rubert, Paweł Niewczas, Jack McAlorum, and Marcus Perry. Preliminary characterization of metal-packaged fiber Bragg gratings under fatigue loading. In *2017 IEEE International Instrumentation and Measurement Technology Conference (I2MTC)*, pages 1–4, 2017.

[13] Y.-J. Rao, 'In-fibre Bragg grating sensors', *Measurement Science and Technology*, vol. 8. p. 355, 1997.

[14] T. Rubert, G. Zorzi, G. Fusiek, P. Niewczas, D. McMillan, J. McAlorum, M. Perry, "Wind turbine lifetime extension decision-making based on structural health monitoring", Renewable Energy, 31 Dec 2019

[15] McAlorum, J., Perry, M., Fusiek, G., Niewczas, P., Mckeeman, I. J. & Rubert, T., "Deterioration of cracks in onshore wind turbine foundations", 12 May 2018 In: Engineering Structures. 167, p. 121-131 11 p.

[16] McKeeman, I.; Fusiek, G.; Perry, M.; Johnston, M.; Saafi, M.; Niewczas, P.; Walsh, M.; Khan, S., "First-time demonstration of measuring concrete prestress levels with metal packaged fibre optic sensors", Smart Materials and Structures, v 25, n 9, p 095051 (10 pp.), Sept. 2016

[17] Perry, M.; Yan, Z.; Sun, Z.; Zhang, L.; Niewczas, P.; Johnston, M., High stress monitoring of prestressing tendons in nuclear concrete vessels using fibre-optic sensors, Nuclear Engineering and Design, v 268, p 35-40, March 2014

[18] Pawel Niewczas and Grzegorz Fusiek. Induction heating assisted optical fiber bonding and sealing technique. page 77536H, 5 2011.

[19] Yoshihiro Yamaguchi, Takashi Kitagawa, Hideki Tanaka, Yasumichi Koshiro, Hideo Takahashi, Shinichi Takezaki, and Masazumi Nakao. Maintenance of Prestressed Concrete Containment Vessels in a Nuclear Power Plant. *Journal of Advanced Concrete Technology*, 14:464–474, 12 2016.

[20] J. McAlorum, 'Structural health monitoring of onshore wind turbine foundations', University of Strathclyde, 2018.

[21] Hoffmann, L., Müller, M., Krämer, S., Giebel, M., Schwotzer, G., & Wieduwilt, T. (01 2007). Applications of fibre optic temperature measurement. *Sci. Eng*, *13*, 363–378.